PB-244 745

ENVIRONMENTAL CHAMBER STUDIES OF ATMOSPHERIC AEROSOLS

D. F. Miller, et al

Battelle Columbus Laboratories

Prepared for:

National Environmental Research Center

December 1973

DISTRIBUTED BY:

NTIS

National Technical Information Service
U. S. DEPARTMENT OF COMMERCE

248010

EPA-650/4-74-009

DECEMBER 1973

PB 244 745

Environmental Monitoring Series

ENVIRONMENTAL CHAMBER STUDIES OF ATMOSPHERIC AEROSOLS

Reproduced by
NATIONAL TECHNICAL
INFORMATION SERVICE
Springfield, Va. 22151

Office of Research and Development
U.S. Environmental Protection Agency
Washington, D.C. 20460

TECHNICAL REPORT DATA

(Please read instructions on the reverse before completing)

1. REPORT NO.	2.	3. RECIPIENT'S ACCESSION NO.
EPA-650/4-74-009		

4. TITLE AND SUBTITLE	5. REPORT DATE
Environmental Chamber Studies of Atmospheric Aerosols	December 1973
	6. PERFORMING ORGANIZATION CODE
7. AUTHOR(S)	8. PERFORMING ORGANIZATION REPORT NO.
D.F. Miller and Arthur Levy	
9. PERFORMING ORGANIZATION NAME AND ADDRESS	10. PROGRAM ELEMENT NO.
Battelle-Columbus Laboratories 505 King Avenue Columbus, Ohio 43201	11. CONTRACT/GRANT NO. 68-02-0574
12. SPONSORING AGENCY NAME AND ADDRESS	13. TYPE OF REPORT AND PERIOD COVERED
ENVIRONMENTAL PROTECTION AGENCY Chemistry and Physics Laboratory National Environmental Research Center Research Triangle Park, North Carolina 27711	14. SPONSORING AGENCY CODE

15. SUPPLEMENTARY NOTES

16. ABSTRACT

The objective of this research program is to obtain data that can be used by EPA to evaluate the role of primary auto-exhaust aerosol in the subsequent formation of photochemical aerosol and to determine what relationships if any might exist between photochemical-aerosol formation and eye irritation. In pursuing the objective, experiments were conducted in which synthetic hydrocarbon-NOx-air mixtures and automobile exhaust-air mixtures were irradiated in a 610-cu-ft smog chamber. Emphasis was placed on strict control of all experimental parameters, on complete detailed analyses of the formation of photochemical aerosols and on the chemistry associated with the formation of other photochemical-smog manifestations, including eye irritation. In addition to obtaining data pertinent to the stated objectives, data were obtained which revealed chemical mechanisms important in aerosol formation and physical mechanisms accounting for losses of aerosols in smog chambers. Among the topics discussed are the experimental results related to the following: (1) Aerosol formation and eye irritation; (2) Mechanisms of aerosol formation in smog and; (3) Influence of primary auto exhaust aerosols on development of secondary aerosols. Automotive exhaust generation and sampling are described in appendix A. Data pertinent to aerosol collections by filtration are presented in appendix B.

17. KEY WORDS AND DOCUMENT ANALYSIS

a. DESCRIPTORS		b. IDENTIFIERS/OPEN ENDED TERMS	c. COSATI Field/Group
Test Chambers	Ozone	Primary auto-exhaust aerosol	13B
Air Pollution	Hydrocarbons		14B
Smog	Nitrogen Oxides	Secondary Aerosols	7D
Aerosol	Sulfur Oxides	Aerosol formation	7E
Collection	Photolysis	Photochemical aerosol	
Eye	Chemical Analysis	Minnesota aerosol analyzing systems	
Humans			

18. DISTRIBUTION STATEMENT	19. SECURITY CLASS (This Report)	21. NO. OF PAGES
		34
	20. SECURITY CLASS (This page)	22. PRICE

EPA Form 2220-1 (9-73)

EPA-650/4-74-009

ENVIRONMENTAL CHAMBER STUDIES OF ATMOSPHERIC AEROSOLS

by

D.F. Miller and Arthur Levy

Battelle-Columbus Laboratories
505 King Avenue
Columbus, Ohio 43201

Contract No. 68-02-0574
Project No. 21 AKB-9
Program Element No. 1AA008

EPA Project Officer: Dr. W.E. Wilson

Chemistry and Physics Laboratory
National Environmental Research Center
Research Triangle Park, North Carolina 27711

Prepared for

OFFICE OF RESEARCH AND DEVELOPMENT
U.S. ENVIRONMENTAL PROTECTION AGENCY
WASHINGTON, D.C. 20460

December 1973

This report has been reviewed by the Environmental Protection Agency and approved for publication. Approval does not signify that the contents necessarily reflect the views and policies of the Agency, nor does mention of trade names or commercial products constitute endorsement or recommendation for use.

ACKNOWLEDGMENTS

The authors gratefully acknowledge D.Y.H. Pui, Dr. K. T. Whitby, and Dr. B. K. Cantrell at the University of Minnesota for their assistance in measuring aerosol size distributions.

The authors also wish to acknowledge their fellow workers who made contributions to this program, especially D. W. Joseph, G. W. Keigley, D. A. Trayser, and G. F. Ward.

Finally, we wish to acknowledge the leadership and interest of Dr. W. E. Wilson, Jr., EPA Project Officer.

TABLE OF CONTENTS

	Page
INTRODUCTION AND OBJECTIVE	1
SUMMARY OF OBSERVATIONS AND CONCLUSIONS	1
EXPERIMENTAL	2
RESULTS	3
Presentation of Data	3
Summaries of Data	8
DISCUSSION	10
Aerosol Formation and Eye Irritation	10
Mechanisms of Aerosol Formation in Smog	10
Physical Processes	11
Chemical Processes	12
Influence of Primary Auto-Exhaust Aerosols on Development of Secondary Aerosols	17
REFERENCES	20

APPENDIXES

A. EXPERIMENTAL METHODS	A-1
B. SUMMARY OF AEROSOL COLLECTIONS	B-1

LIST OF TABLES

Table 1.	Summary of Results of Smog-Chamber Experiments	9
Table 2.	Correlations Between Eye Irritation and Various Independent Variables	11
Table B-1.	Summary of Aerosol Collections by Filtration	B-1

Preceding page blank

FINAL REPORT

on

ENVIRONMENTAL CHAMBER STUDIES OF ATMOSPHERIC AEROSOLS

to

U.S. ENVIRONMENTAL PROTECTION AGENCY

from

BATTELLE
Columbus Laboratories

December 12, 1973

INTRODUCTION AND OBJECTIVE

The objective of this research program is to obtain data that can be used by EPA to evaluate the role of primary auto-exhaust aerosol in the subsequent formation of photochemical aerosol and to determine what relationships if any might exist between photochemical-aerosol formation and eye irritation. In pursuing the objective, experiments were conducted in which synthetic hydrocarbon-NO_x-air mixtures and automobile exhaust-air mixtures were irradiated in a 610-cu-ft smog chamber. Emphasis was placed on strict control of all experimental parameters, on complete detailed analyses of the formation of photochemical aerosols* and on the chemistry associated with the formation of other photochemical-smog manifestations, including eye irritation. In addition to obtaining data pertinent to the stated objectives, data were obtained which revealed chemical mechanisms important in aerosol formation and physical mechanisms accounting for losses of aerosols in smog chambers.

SUMMARY OF OBSERVATIONS AND CONCLUSIONS

In addition to this report, three papers have been presented which describe various aspects of the program. The papers are entitled, "Aerosol Formation in Photochemical Smog: The Effect of Humidity and Small Particles"[1], "Evolution of the Freeway Aerosol"[2], and "Effect of Stirring on Aerosol Production in a Smog Chamber"[3]. A fourth paper entitled "The Size Distribution and Concentration of Combustion and Photochemical Aerosols Attributable to Automobiles"[4] will be presented at the 67th Annual Meeting of the Air Pollution Control Association, June, 1974.

*In this report, the term photochemical aerosols refers to aerosols (condensed matter) which form as a result of photochemically induced reactions occurring in the smog chamber.

Although these papers discuss many of the results of this program, several other important observations were made while assembling and perusing these data. The observations are listed below, together with some of the conclusions contained in the papers cited. Observations not referenced are discussed in the text of this report.

- There is no substantial relationship between the severity of eye irritation and the amounts of aerosols formed photochemically.

- Inclusion of primary aerosols during the formation of photochemical aerosols changes the size distribution of the resulting aerosol and may have a sizable influence on light scattering and visibility reduction. However, the presence of primary aerosols appears to have little effect on the volume of aerosol material produced by the photochemical processes.

- Losses of aerosols to chamber surfaces agree with diffusion-rate theory for various-size particles. However, turbulence created by mechanically stirring the chamber's atmosphere increases the loss rate by factors as large as 5, and the loss rates differ for aerosols of different chemical compositions.[3]

- The relationships between aerosol mass concentration inferred from size-distribution data, aerosol mass concentration determined gravimetrically, and aerosol mass concentration predicted by total light scattering are fairly consistent and rarely differ by factors greater than 2.[4]

- Patterns of photochemical-aerosol formation from aromatic hydrocarbon-NO_x-air and automobile exhaust-air mixtures are similar, and OH radicals appear to be important precursor intermediates for aerosol formation in these cases. With olefinic hydrocarbon-NO_x-air and olefinic hydrocarbon-NO_x-SO_2-air mixtures, photochemical-aerosol formation appears to depend on ozone concentrations.

- The initial concentration of aerosols emitted by automobiles is very high and the aerosol sizes are quite small (~0.02 μm diameter). Under most laboratory conditions, the small aerosols coagulate quite rapidly unless rapid and extensive dilution is applied.[4]

- TEL motor-fuel additive has no pronounced effect on the rate of NO photo-oxidation or on other photochemical-smog manifestations, including eye irritation.

Presumably, additional important information can be derived from the data furnished in this report. Chemical models of the smog-chamber data or chemical analyses of the numerous aerosol collections may, for example, lead to an improved understanding of aerosol development in smog.

EXPERIMENTAL

Battelle-Columbus' 610-cu-ft smog chamber has been described previously.[5] Light-intensity measurements by NO_2 photolysis[6] and o-nitrobenzaldehyde photolysis[7] agree quite well, as described by Gordon.[8] The value for k_d is ~0.45 min^{-1}. Total hydrocarbon was determined by

flame ionization, specific hydrocarbons by flame-ionization gas chromatography, CO by NDIR, SO_2 by flame photometry and a coulometric analyzer, O_3 by chemiluminescence with ethylene, NO and NO_2 by automated Saltzman using a dichromate oxidizer for NO, PAN by electron-capture gas chromatography, and light scattering by broad-band (420 to 570 nm) integrated nephelometry. Measures of eye irritation were made by three 7-member eye-panel teams chosen from Battelle-Columbus' staff. Selection and screening of the panelists are described in Appendix A.

Aerosol size distributions were obtained using the Minnesota Aerosol Analyzing System (MAAS) developed by Dr. K. T. Whitby and his colleagues at the University of Minnesota. Instruments comprising the MAAS are a portable electrical-mobility analyzer, a modified optical particle counter, and a condensation nuclei counter. Calibration and operation of this system in determining size distributions has been reported by Whitby et al.[9]

Synthetic automobile exhausts used as part of the total exhausts in Runs AA-032 through AA-038 were made up of 50 percent by weight of the respective motor fuel (simulating fuel-derived exhaust constituents) and 50 percent by weight of a C_2-C_4 hydrocarbon mixture (simulating combustion-derived exhaust constitutents). The percentage composition of the combustion mixture was ethane 4.0, ethylene 44.1, acetylene 28.0, propylene 16.0, 1-butene 6.2, and trans-2-butene 1.7.

Procedures for operating the automobiles and transferring exhausts to the smog chamber are described in Appendix A.

RESULTS

Presentation of Data

A major requirement of this program was to furnish EPA a comprehensive copy of data emanating from the aerosol and chemical measurements made during smog-chamber experiments. Because of the large amount of data obtained, a separate Data Report was prepared containing:

(1) Time-concentration profiles of the gas-phase chemistry of each smog experiment

(2) Computer tabulated printouts of experimental conditions and rates of change of various constituents during each experiment

(3) Time-concentration profiles of various aerosol parameters inferred from aerosol size distributions measured during the experiments

(4) Computer-generated plots of the changes in aerosol surface distributions with irradiation time

(5) Tabulations of the response times to eye irritation for each panelist, and the arithmetic and geometric mean times for each experiment.

Two copies of the Data Report were delivered to EPA together with this report. Examples of the gas-phase and aerosol profiles appearing in the Data Report are shown in Figures 1 through 4.

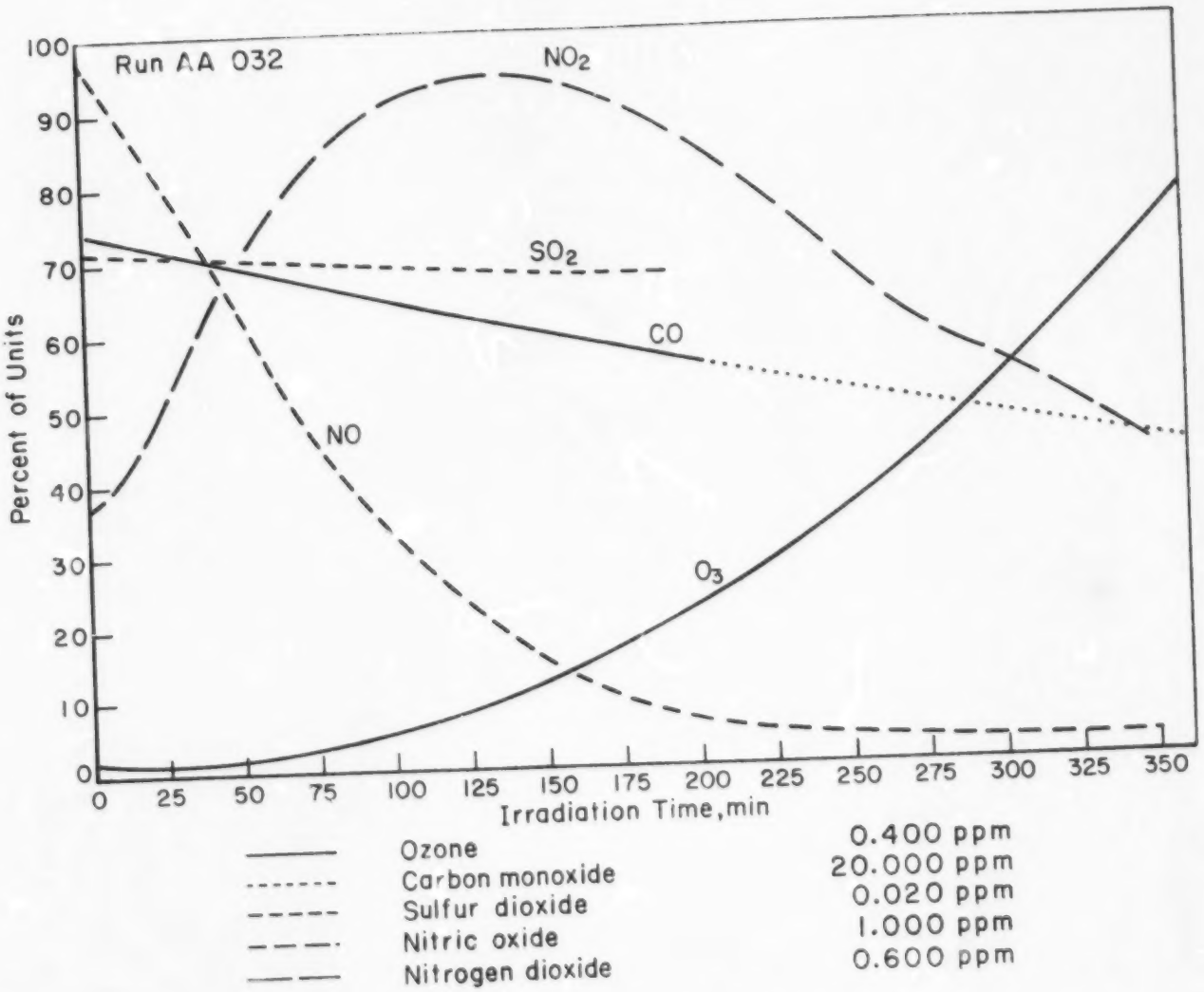

FIGURE 1. SMOG PROFILE OF INORGANIC GASES

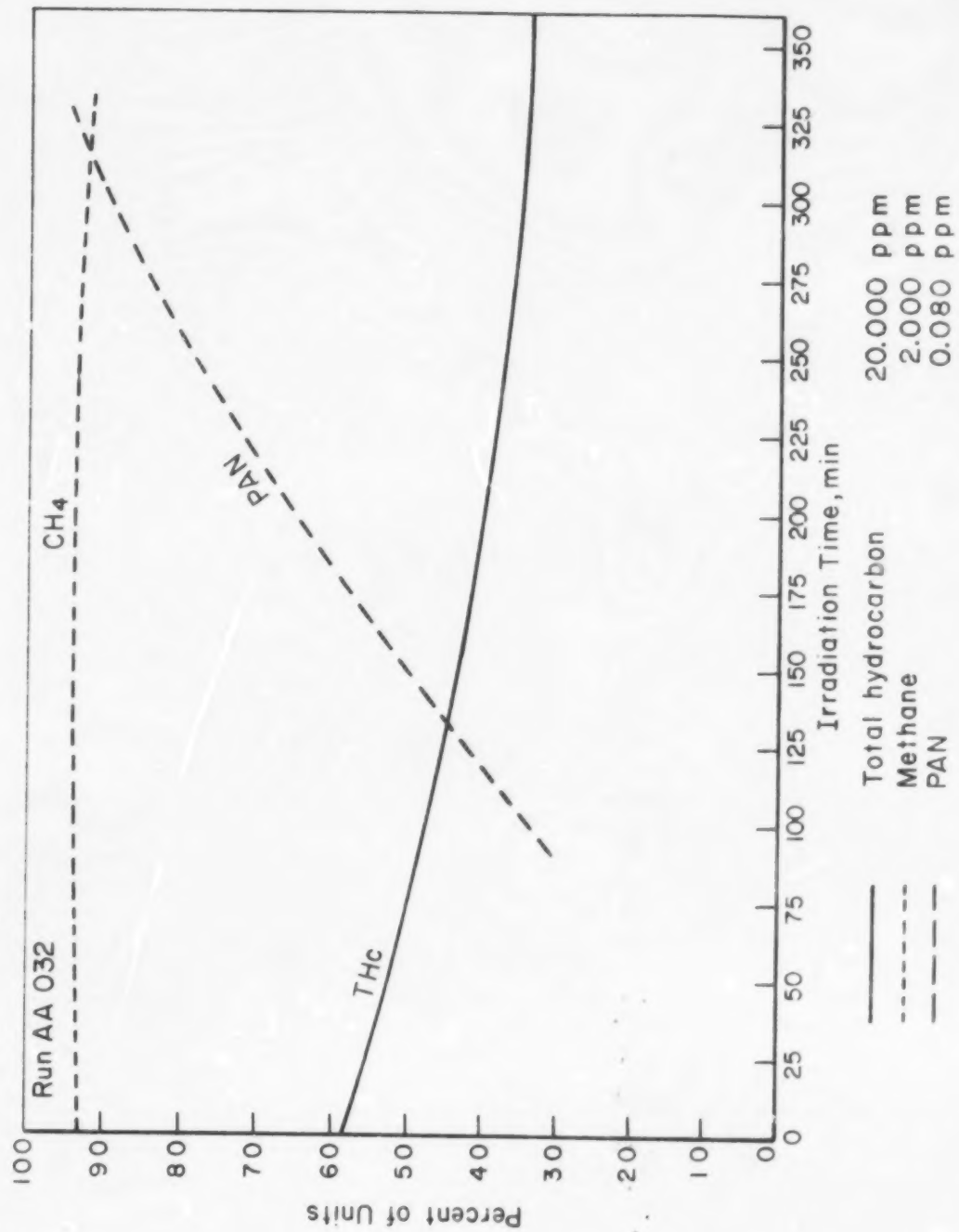

FIGURE 2. SMOG PROFILE OF ORGANIC GASES

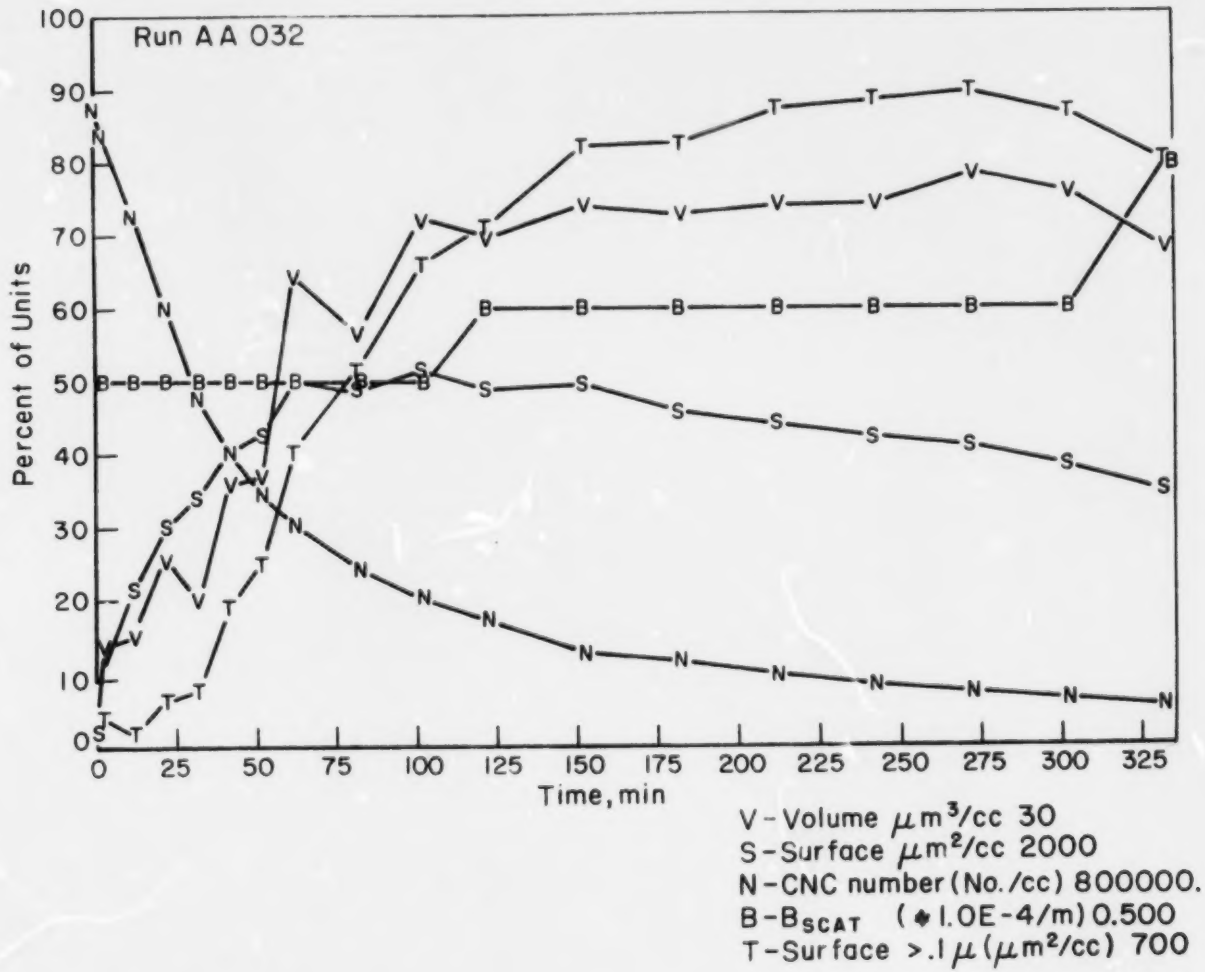
Run AA 032
Percent of Units
Time, min
V - Volume μm³/cc 30
S - Surface μm²/cc 2000
N - CNC number (No./cc) 800000.
B - B_SCAT (♦ 1.0E-4/m) 0.500
T - Surface >.1 μ (μm²/cc) 700

FIGURE 3. SMOG PROFILE OF INTEGRATED LIGHT SCATTERING (B_{SCAT}) AND VARIOUS AEROSOL PARAMETERS COMPUTED FROM SIZE-DISTRIBUTION MEASUREMENTS

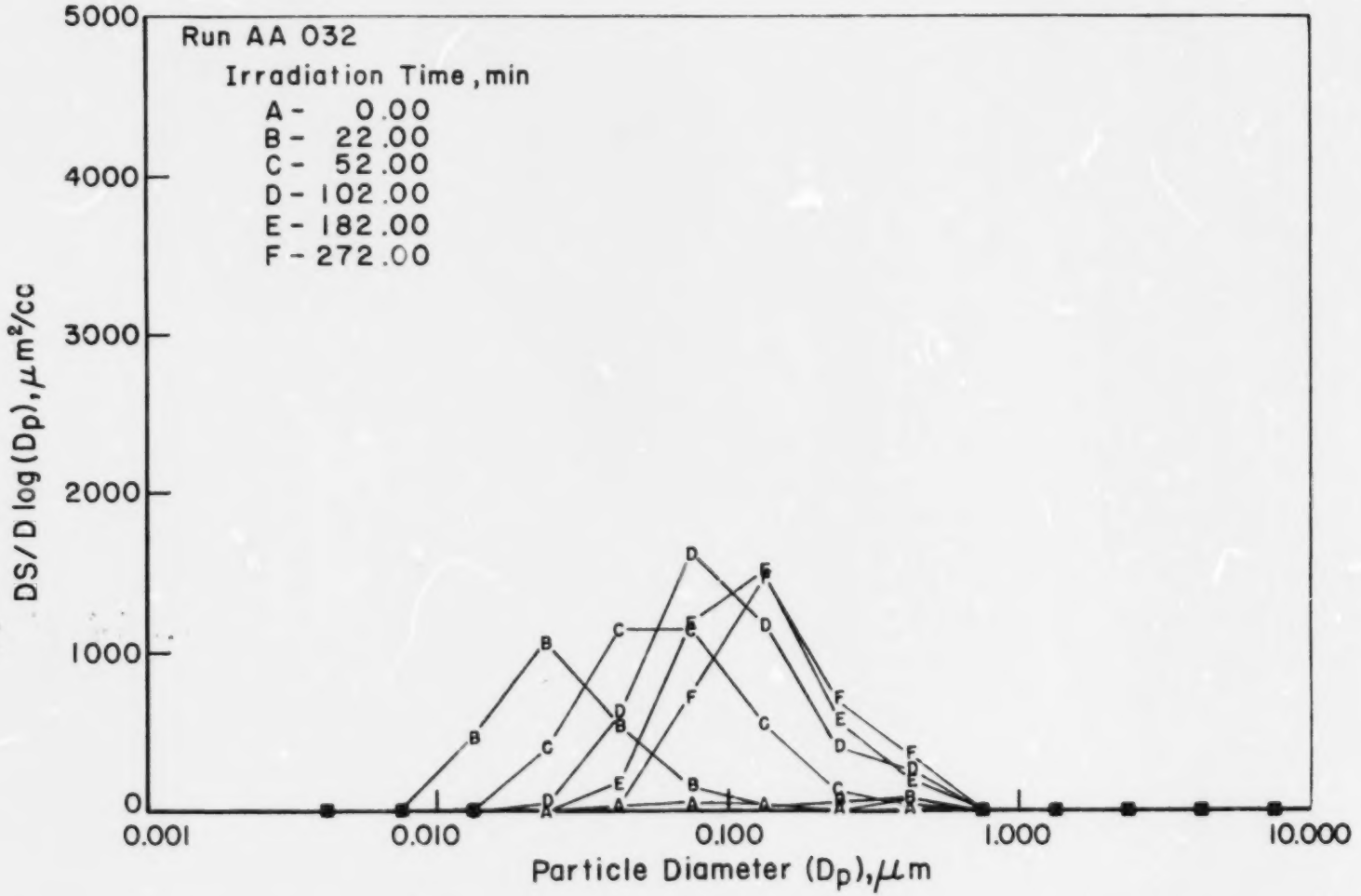

FIGURE 4. CHANGES IN AEROSOL SURFACE DISTRIBUTION AS A FUNCTION OF IRRADIATION TIME

Figures 1 through 4 describe results from an experiment where filtered auto exhaust (nonleaded fuel) was irradiated for 6 hours. Just before irradiation, condensation nuclei were added to the chamber. In Figure 1, the loss rate of SO_2 is shown to be less than the dilution rate (indicated by the CO curve). This apparent anomaly reflects the inaccuracy of the SO_2 monitor at very low concentrations (<0.02 ppm). In Figure 2, no loss of methane is indicated because the purified air used to make up volume losses contains methane. In Figure 3, the number concentration of aerosols is greatest at 0 minutes because of the addition of condensation nuclei (CN) prior to irradiation. Although the number concentration is high (7×10^5 cm^{-3}) at t = 0 minutes, the initial amount of aerosol surface due to CN is small (~50 $\mu m^2 cm^{-3}$), as indicated in Figures 3 and 4. In this case, the added CN had little effect on the development of the photochemically derived aerosols.

Aerosol Mass and Chemical Data. Numerous aerosol collections were made at the end of the irradiation periods (4 to 6 hours). Aerosols were collected on a variety of filter media for mass determinations and/or subsequent chemical analyses. Data pertinent to these collections are presented in Table B-1, Appendix B.

Computer Tape Record. In addition to the Data Report, a 7-track IBM compatible magnetic tape was prepared containing all gas-phase data converted to engineering units. The tape was delivered to the Project Officer, September 26, 1973.

EPA-CRC CAPE-19 Study. As an adjunct to this program, a number of aerosol analyses using the MAAS were conducted to characterize the aging process of primary automobile particulate in a dark residence chamber. Those analyses were performed in conjunction with the EPA-CRC CAPE-19 program at BCL. Copies of those data, tabulated and graphically displayed by computer, were delivered to the Project Officer, April 6, 1973.

Summaries of Data

Initial experimental conditions and results of all the smog-chamber experiments are summarized in Table 1. Less familiar abbreviations are defined below:

% RH = percent relative humidity

b_{scat} = extinction coefficient of light scattering

S_T = total aerosol surface concentration

V_T = total aerosol volume concentration

Mass = aerosol mass concentration determined by filtering and weighing

PAN = peroxyacetylnitrate

HCHO = formaldehyde

RCHO = total aldehyde.

TABLE 1. SUMMARY OF RESULTS OF SMOG-CHAMBER EXPERIMENTS[a]

		Initial Concentrations and Conditions									Maximum or Final Concentrations								
		Gases						Aerosols		Stirring	Gases				Aerosols				Eye Irritation as
Run	Hydrocarbons, ppm C	H_2O, % RH	CO, ppm	NO, ppm	NO_2, ppm	SO_2, ppm	O_3, ppm	b_{scat}, $10^{-4}m^{-1}$	S_T, $\mu m^2 cm^{-3}$	Speed, rpm	O_3, ppm	PAN, ppm	HCHO, ppm	RCHO, ppm	b_{scat}, $10^{-4}m^{-1}$	S_T, $\mu m^2 cm^{-3}$	V_T, $\mu m^3 cm^{-3}$	Mass, $\mu g\ m^{-3}$	Response Time, sec
AA 005	Toluene, 46.6	66	<3	1.10	1.00	0.00	0.00	0.2	–	0	0.55	0.30	0.1	1.1	82	–	–	921	77
AA 006	Toluene, 46.3	58	<3	0.98	0.98	0.00	0.00	0.2	<10	0	0.45	0.40	0.1	1.3	100	9,274	640	1,100	56
AA 007	Toluene, 46.9	66	<3	0.94	0.94	0.00	0.00	0.2	<10	990	0.53	0.43	0.1	1.4	21	1,566	205	278	47
AA 008	1-heptene, 35.8	66	<3	0.72	0.75	0.00	0.00	0.2	<10	0	0.64	0.05	1.3	4.8	13	7,123	352	180	46
AA 009	1-heptene, 20.3	66	<3	0.72	0.72	0.00	0.00	0.2	<10	0	0.64	0.07	0.6	2.8	1.7	2,196	90	67	84
AA 010	1-heptene, 34.6	70	<3	0.70	0.70	0.00	0.00	0.2	–	1,000	0.62	0.01	1.2	5.1	0.9	3,042	100	80	61
AA 011	Benzene, 30.8	70	<3	0.71	0.72	0.00	0.00	0.2	<10	0	0.00	–	0.0	0.3	2.9	2,316	102	117	189
AA 012	Toluene, 16/mesitylene, 28	66	<3	0.68	0.69	0.00	0.00	0.2	<10	0	0.98	0.20	0.4	2.2	21	8,452	443	327	83
AA 013	Benzene, 32.1	66	75	0.75	0.75	0.00	0.00	0.2	<10	0	0.16	–	0.0	0.2	2.1	2,013	89	–	199
AA 015	Benzene, 31.8	62	<3	0.73	0.71	0.10	0.00	0.2	<10	0	0.00	–	0.0	0.0	5.8	4,019	198	140	198
AA 016	–	58	<3	<0.05	0.00	0.19	0.00	0.2	<10	0	0.06	–	–	–	6.5	6,372	234	174	–
AA 017	–	14	<3	<0.05	0.00	0.23	0.00	0.2	<10	0	0.00	–	–	–	1.7	2,904	117	–	218
AA 018[b]	–	66	<2	0.20	2.00	0.60	0.60	0.2	<10	0	–	–	–	–	0.2	1,478	28	–	–
AA 019[b]	Propylene, 9.0	70	<3	<0.05	0.00	0.96	0.72	0.2	<10	0	–	–	–	–	12	17,580	519	263	–
AA 020	α-pinene, 27.4	70	<3	0.73	0.76	0.00	0.00	0.2	<10	0	0.44	–	–	–	>100	>20,000	>2,000	–	97
AA 021[b]	1-heptene, 20.0	78	<3	<0.05	–	0.00	0.64	0.2	<10	0	–	–	–	–	2.8	7,553	248	65	–
AA 022[b]	1-heptene, 20.8	78	<3	<0.05	–	0.51	0.51	0.2	<10	0	–	–	–	–	20	>20,000	> 600	281	188
AA 023[c]	Toluene, 18.3	62	<3	0.76	0.73	0.00	0.00	0.2	100	0	0.42	0.25	0.1	0.9	20	5,592	316	456	92
AA 024	Auto exhaust, 16.0	55	225	2.00	0.48	0.06	0.00		1,292	0	0.52	0.25	0.5	1.8	6	3,353	157	165	88
AA 025[d]	Auto exhaust, 15.0	58	245	1.40	0.89	0.01	0.00	0.2	<10	0	0.78	0.49	0.5	1.8	2	3,542	114	125	104
AA 028	1-heptene, 12.0,	66	<3	0.43	0.01	0.06	0.00	0.2	<10	0	0.39	–	0.3	1.4	0.9	3,028	77	102	103
AA 029	1-heptene, 12.1	74	<3	0.48	0.01	0.06	0.00	0.2	<10	1,000	0.37	–	0.3	1.3	0.6	2,470	67	84	92
AA 030	1-heptene, 11.2	66	<3	0.52	0.01	0.00	0.00	0.2	<10	0	0.51	–	0.3	1.3	0.3	509	9	52	118
AA 031[c]	1-heptene, 11.7	70	<3	0.50	0.01	0.00	0.00	0.3	100	0	0.39	–	0.3	1.4	0.3	461	12	62	92
AA 032[c,d]	Auto exhaust, 8.0	62	15	0.97	0.22	<0.01	0.00	0.2	50	0	0.26	0.07	0.3	1.0	0.4	1,030	24	58	126
AA 033	Auto exhaust, 8.1	62	40	0.72	0.06	<0.01	0.00	0.2	60	0	0.53	0.19	0.3	1.2	0.4	1,116	25	58	104
AA 034[d]	Auto exhaust, 8.2	58	41	0.78	0.16	<0.01	0.00	0.2	<10	0	0.54	0.17	0.4	1.1	0.4	756	16	47	114
AA 035[e]	Auto exhaust, 8.1	66	39	0.73	0.02	<0.01	0.00	0.3	512	0	0.46	0.22	0.3	1.1	0.5	877	27	43	107
AA 036[e]	Auto exhaust, 8.1	58	40	0.79	0.01	<0.01	0.00	0.3	433	0	0.50	0.23	0.4	1.2	0.5	827	25	38	138
AA 037[d,e]	Auto exhaust, 8.0	58	42	0.77	0.09	<0.01	0.00	0.2	<10	0	0.57	0.29	0.3	1.2	0.3	755	16	42	94
AA 038[d,e]	Auto exhaust, 8.2	58	40	0.78	0.09	<0.01	0.00	0.2	<10	0	0.45	0.27	0.3	1.2	0.3	670	15	46	103

[a] Abbreviations defined on page 8.
[b] Dark reactions.
[c] Condensation nuclei added before irradiation.
[d] Auto exhaust filtered of primary aerosol.
[e] Leaded fuel; all other exhaust experiments made with unleaded fuel.

DISCUSSION

Aerosol Formation and Eye Irritation

One of the objectives of this program was to determine whether a relationship exists between the degree of eye irritation and the concentration of photochemically generated aerosols. The procedure for determining eye irritation was to expose two groups of panelists (totaling 14 persons) to the chamber contents about 2 hours after the NO_2 concentration passed through its maximum. Typically, during this period of irradiation, aerosol surface and volume concentrations also reached or passed through their maximum values. It has been established on the EF-8 project for API that this period of irradiation coincides with maximum eye irritation, at least where auto exhausts are irradiated.[10] More details on the eye-panel selection and testing are given in Appendix A.

Arithmetic and geometric mean response times and response indices are presented in the supplementary Data Report. Individual responses of each panelist are also provided there for any additional statistical analyses EPA may want to conduct.

In comparing eye-irritation intensities between pairs of experiments in which aerosol concentration was the only widely varying parameter (Table 1, Runs: AA-006 and AA-007, AA-008 and AA-010, AA-016 and AA-017, and AA-028 and AA-029), it appears that the amount of aerosol surface and/or volume has very little or no influence on eye irritation. To more fully explore any possible relationship between these variables, linear regression equations with two variables were obtained (by method of least squares), and correlation analyses were performed to describe the strength of the regression equations. Regression equations and correlations were obtained with eye irritation (100/mean response time, sec) as the dependent variable and PAN (ppm), formaldehyde (ppm), and total aldehyde (ppm) as independent variables in addition to aerosol surface ($\mu m^2/cm^3$) and aerosol volume ($\mu m^3/cm^3$) concentrations. Values of the independent variables were taken near the times of the eye-irritation measurements. The results are shown in Table 2. As indicated by the correlation coefficients in Table 2, there is virtually no correlation between eye irritation and aerosol or PAN concentrations, and only moderate correlation between eye irritation and aldehyde concentrations. In conclusion, neither the concentration of aerosols nor the concentration of certain gaseous products, taken individually, correlated highly with eye irritation associated with photochemical smog arising from irradiation of typical hydrocarbon-NO_x and hydrocarbon-NO_x-SO_2 mixtures in air.

Mechanisms of Aerosol Formation in Smog

Use of the MAAS has revealed several important features regarding aerosol formation in smog which have been previously obscured because of inadequate aerosol-analyzing methods. Most important, perhaps, these measurements lead to a clearer understanding of aerosol growth processes, which in turn enables us to speculate on the chemical mechanisms prevailing in aerosol formation. Before discussing aerosol chemistry, it is instructive to describe the physical pattern of aerosol formation as it occurs in a smog chamber operating as a batch reactor.

TABLE 2. CORRELATIONS BETWEEN EYE IRRITATION AND VARIOUS INDEPENDENT VARIABLES

Independent Variable	Linear Regression Parameter			Correlation Coefficient
	Number of Observations	Slope	Intercept	
Aerosol surface concentration	26	−0.01	0.96	−0.08
Aerosol volume concentration	26	−0.01	0.96	−0.12
Formaldehyde concentration	24	0.55	0.75	0.40
Total aldehyde concentration	24	0.21	0.62	0.58
PAN concentration	17	0.51	0.95	0.14

Physical Processes

Profiles of some of the parameters associated with aerosol formation during the irradiation of filtered and diluted auto exhaust are presented in Figure 5. As indicated here, there is a very rapid increase in the aerosol number immediately after irradiation is initiated. The very brief induction period is the time required for the vapor of the incipient aerosols to reach critical concentrations at which nucleation begins. Once formed, the nuclei begin to coagulate. The maximum in the total number of nuclei occurs when the rate of coagulation equals the rate of nucleation. Beyond this point, the rate of nucleation diminishes as more surface becomes available to support condensation — thermodynamically a more favorable process. Thus, shortly after the maximum in the total-number curve, condensation is believed to be the prevailing mechanism by which aerosol volume increases. In this experiment, total aerosol production (total-volume curve) increases linearly for about 1 hour and then diminishes. The decrease in the volumetric conversion rate is generally attributed to (1) decreases in concentrations of precursor constituents, (2) wall losses, and (3) chamber dilution.

Increases in the concentration of total surface area result from nucleation and from condensation of new vapor on existing aerosols. At the same time, however, coagulation reduces the total aerosol surface. For the experiment depicted in Figure 5, after about 1 hour, the rate at which surface is destroyed by coagulation is greater than the rate at which new surface is created by condensation.

Integrated light scattering (b_{scat}) is seen to increase throughout most of the irradiation, leveling off only during the last hour. The fact that the slope of the total-volume curve after 2 hours of irradiation is less negative than the slope of the total-surface curve indicates that the increase in light scattering after 2 hours is due primarily to coagulation of small aerosols produced earlier in the reaction.

As mentioned previously, similar plots of total aerosol number, total volume, total-surface-area concentrations, and integrated light scattering versus irradiation time are available in the supplementary Data Report for each experiment.

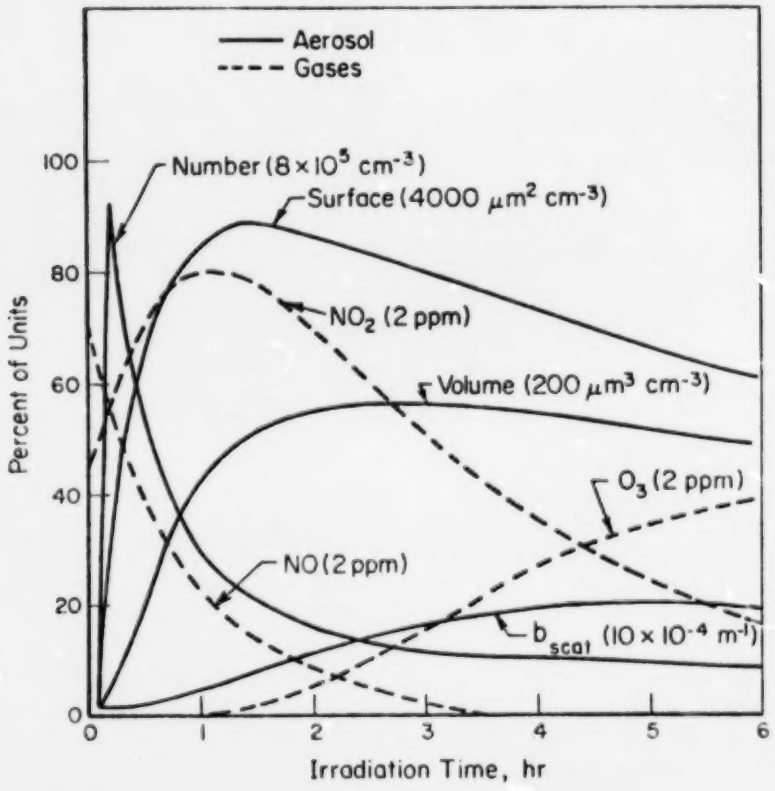

FIGURE 5. PROFILE OF AEROSOL FORMATION DURING IRRADIATION OF FILTERED AND DILUTED AUTO EXHAUST (16 PPM C HYDROCARBONS)

Chemical Processes

Many investigators have been under the impression that the formation of aerosols in smog is directly related to the formation of ozone as evidenced by the correspondence in the appearance of light scattering and ozone. Our findings indicate that such dependency is observed only for olefin-NO_x and olefin-NO_x-SO_2 smog systems, the latter resulting primarily in formation of sulfate aerosol.

In aromatic hydrocarbon-NO_x systems, this dependency is not observed and an alternative dependence involving OH is suggested.

Oxidation of Hydrocarbons. When diluted auto exhaust is irradiated in the smog chamber, most of the aerosol volume is produced during the period of NO to NO_2 conversion, as illustrated in Figure 5. In an earlier study of the propensity of specific exhaust hydrocarbons to generate photochemical aerosols, aromatic compounds stood out as being far more reactive than most olefin or paraffin compounds.[11] Thus the pattern of aerosol formation observed during auto exhaust irradiation would be expected to appear during irradiation of aromatic hydrocarbon-NO_x-air mixtures.

Figure 6 shows the formation of aerosol during irradiation of toluene and NO_x in air (Run AA-008). In this case it is quite clear that aerosol production occurs almost exclusively during the NO to NO_2 conversion period. The abrupt decline in aerosol production at 240 minutes cannot be attributed to the consumption of toluene but may be associated with the consumption of NO. When one examines kinetic data for reactions of aromatic hydrocarbons with the free radicals in smog[12], it is clear that OH is the most important attacking species. Furthermore, recent kinetic simulations of smog chemistry[13] reveal that, of the OH-forming reactions listed below, the overall rate for Reaction (1) is much greater than that for all the others, unless, of course, the NO concentration is very small.

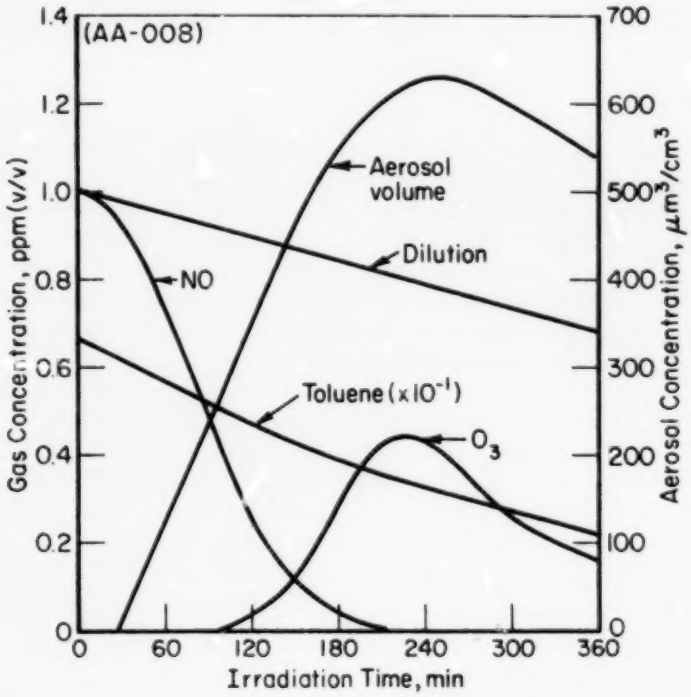

FIGURE 6. AEROSOL-FORMATION PROFILE DURING IRRADIATION OF TOLUENE-NO_x-AIR MIXTURE

Thus Reaction (1) serves to continually pump OH into the system to react with aromatic hydrocarbons while also oxidizing NO to NO_2. When the concentration of NO becomes very small, other intermediates (e.g., O atoms, RO_2 RO, and HO_2 radicals) become competitive in reacting with aromatics, and presumably the nature and/or rate of these reactions do not lead to substantial aerosol yields.

$$HO_2 + NO \rightarrow HO + NO_2 \qquad (1)$$

$$HONO + h\nu \rightarrow HO + NO \qquad (2)$$

$$H_2O_2 + h\nu \rightarrow 2HO \qquad (3)$$

$$O(^1D) + H_2O \rightarrow 2HO \qquad (4)$$

$$RCHO_2H \rightarrow RCHO + HO \qquad (5)$$

Although most paraffins and low molecular-weight olefins yield much less organic aerosol than aromatics, olefins possessing ≥4 carbon atoms produce substantial quantities when irradiated with NO_x. For example, 1-heptene yields about 50 to 70 percent of the amount of aerosol generated by equal concentrations of toluene.

The reaction between olefins and ozone appears to be the most important in forming these aerosols. As shown in Figure 7, substantial aerosol formation does not occur during NO oxidation (where the OH concentration is highest), but rather after NO is consumed and O_3 is generated. Thus, unlike the situation with aromatic hydrocarbons, aerosol formation from the higher-molecular-weight olefins seems to involve reactions with O_3. Results of the dark reaction of O_3 with 1-heptene (Run AA-021) support the belief about the importance of O_3 in the irradiation experiment.

SO_2 Oxidation. Numerous studies have been conducted to ascertain the interaction of SO_2 in photochemical smog, with particular concern for the formation of sulfuric acid aerosols. Although it has been well established that sulfuric acid aerosols are indeed products of SO_2 oxidation, considerable uncertainty exists as to the rate of SO_2 oxidation and the prevailing mechanisms involved. In most studies where SO_2 has been irradiated in air containing hydrocarbons and nitrogen oxides, no quantitative results have been reported for SO_2-oxidation products. Thus it has not been clear as to the extent to which the observed losses of SO_2 in these systems actually culminated in sulfuric acid aerosols.

Recently Cox and Penket[14] conducted a series of *dark* reactions in which SO_3 was successfully monitored by means of radiochemical techniques. Clark and Whitby[15] determined, indirectly, the rate of SO_3 formation from SO_2 oxidation by measuring aerosol products with the same instrumentation employed in this study. In their experiments, SO_2 was irradiated in the absence of other pollutants. Similarly in this study, irradiation experiments were carried out with SO_2 added to air otherwise unintentionally contaminated (Runs AA-016 and AA-017), but also to air to which hydrocarbons and NO_x were intentionally added (Runs AA-015, AA-028, and AA-029). In the "SO_2-clean air" runs, humidity was the independent variable.

Figure 8 shows the effect of humidity on the aerosol volumetric formation rate (dV/dt) when SO_2 was irradiated alone in air. At 58 percent RH, maximum dV/dt was about three times greater than that at 14 percent RH. It is of considerable interest to determine whether the aerosol-formation rates observed in these experiments can be substantiated on the basis of SO_2 oxidation and aqueous sulfuric acid vapor-pressure data.[16] If one assumes that the loss of SO_2 is due entirely to SO_3 formation, and further that equilibrium exists between the condensed and vapor phases of aqueous sulfuric acid, $SO_3(H_2O)_x$, then the observed decay in SO_2 should be equal to the observed production of $SO_3(H_2O)_x$ aerosol. The appropriate calculation for predicting the change in aerosol volume due to SO_2 oxidation is shown below for Run AA-016:

$$\Delta[V_{SO_3(H_2O)_x}]/\Delta t = \frac{\Delta[SO_2]/\Delta t}{x\rho\, r}, \qquad (6)$$

where x = mole fraction of $SO_3 \cdot H_2O$ in $SO_3(H_2O)_x$ at the temperature and humidity of the system

ρ = density of $SO_3(H_2O)_x$ at the same conditions

r = ratio of molecular weight of SO_2 to $SO_3 \cdot H_2O$.

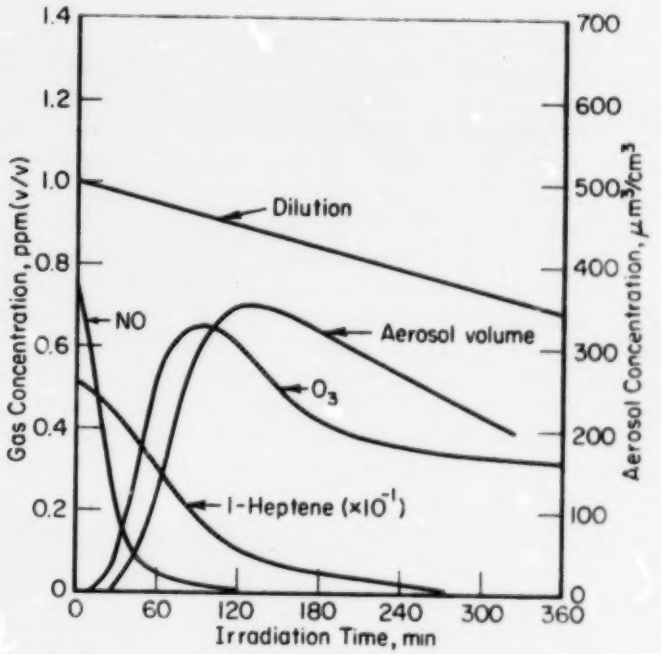

FIGURE 7. AEROSOL-FORMATION PROFILE DURING IRRADIATION OF 1-HEPTENE-NO_x-AIR MIXTURE

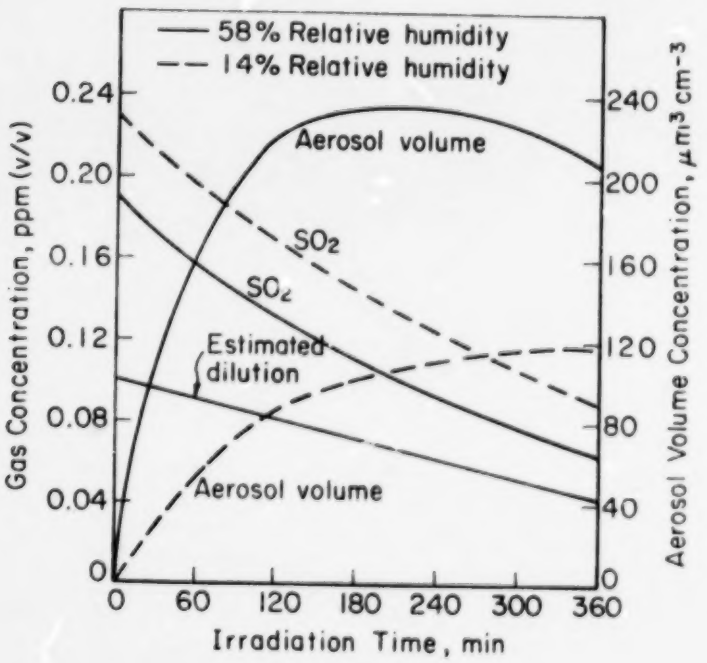

FIGURE 8. EFFECT OF HUMIDITY ON THE VOLUME OF H_2SO_4 AEROSOL FORMED DURING IRRADIATION OF SO_2-AIR MIXTURES

To simplify the calculation, the change in aerosol volume was predicted over the irradiation interval of 0 to 60 minutes where rates were approximately linear. For the conditions of Run AA-016, the constants in Equation (6) are: x = 0.40, ρ = 1.3 g/cm^3, and r = 0.65. Actual SO_2 loss during the first hour (corrected for dilution) was 0.019 ppm. Using the units conversion factor, 1 ppm SO_2 = 2610 μg/m^3 (25 C, 1 atm), the calculated value for $V_{SO_3(H_2O)_x}$ at 60 minutes is 147 μm^3/cm^3. The observed value was about 160 μm^3/cm^3. Performing the same type of calculation on results of Run AA-017 (where ΔSO_2 = 0.015 ppm, x = 0.61, ρ = 1.5 g/cm^3, r = 0.65) leads to a prediction for $V_{SO_3(H_2O)_x}$ of 66 μm^3/cm^3. The observed value was 60 μm^3/cm^3. The good agreement in these instances supports the hypothesis that the observed decay in SO_2 was indeed due to *gas-phase oxidation* of SO_2 to SO_3 rather than to either absorption or heterogeneous reactions of SO_2 on chamber surfaces. What is difficult to explain is the observed rate of SO_2 oxidation. The rates in Runs AA-016 and AA-017 ranged from about 7 to 10 percent/hr. The maximum theoretical rate for conditions of this study is less than 2 percent/hr.[16] One is therefore left with the conclusion that contamination is responsible for the enhanced rate, but at contaminate concentrations <2 ppm C "nonreactive" hydrocarbon and < 0.05 ppm NO_x. Clark and Whitby[15] also suspected that contamination may have increased SO_2 oxidation rates observed in their work, although the oxidation rates they calculated were within the theoretical limit, even when contamination was suspected.

Figure 9 shows the results of SO_2 oxidation and subsequent $SO_3(H_2O)_x$ aerosol formation when 0.06 ppm SO_2 was irradiated in air to which 1-heptene and NO_x were intentionally added. (The aerosol-volume profile is also indicated in Figure 9 for 1-heptene/NO_x irradiation in the absence of SO_2.) Unlike the results of irradiating SO_2 in clean air, there is a substantial delay before reaching the maximum rate of aerosol formation, which is also coincident with the maximum formation rate for ozone.

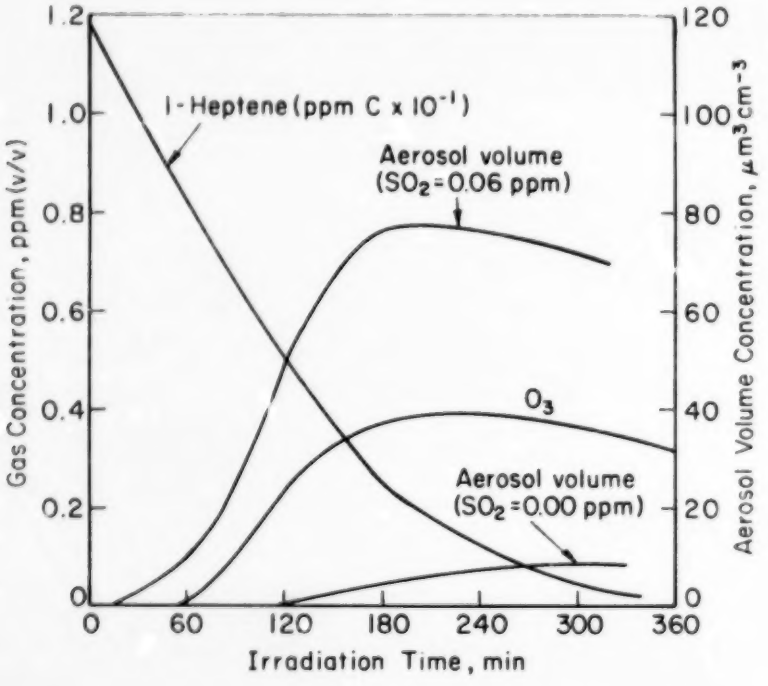

FIGURE 9. AEROSOL FORMATION PROFILE DURING IRRADIATION OF 1-HEPTENE-NO_x-AIR MIXTURES IN PRESENCE AND ABSENCE OF SO_2

Several investigators, including Cox and Penkett[14], argue that the most likely mechanism for SO_2 oxidation under these conditions involves oxidation via zwitterions produced from ozonolysis of 1-heptene. A reasonable extension of the theory is the presumption that the SO_2 oxidation rate, or $SO_3(H_2O)_x$ formation rate, would be first order in each of three reactants (SO_2, O_3, and 1-heptene) as indicated by Equation (7).

$$d\ SO_3(H_2O)_x/dt = k\cdot(SO_2)\cdot(O_3)\cdot(1\text{-heptene}) . \qquad (7)$$

During the period from 90 to 150 minutes where $d\ SO_3(H_2O)_x/dt$ was nearly constant, the product of the concentration terms would be expected to be constant. Inserting the appropriate values of SO_2, O_3, and 1-heptene at irradiation times of 90, 120 and 150 minutes yields products of 0.38, 0.46, and 0.40 ppm^3, respectively, and the first-order assumption appears valid. However, the abrupt decrease in dV/dt near 200 minutes severely contradicts predictions based on this first-order scheme. At 200 minutes, the $[O_3][SO_2][olefin]$ product was 0.23 ppm^3, which would indicate an aerosol-formation rate of about half the maximum (4 $\mu m^3 cm^{-3}\ min^{-1}$), and not zero. Reasons for the abrupt change in slope of the aerosol-volume curve at 180 to 200 minutes are not apparent. It was not due to aerosol losses because at this time the mean aerosol diameter was about 0.1 μm – a size that is not especially susceptible to wall loss due to diffusion or settling.

The maximum rate of SO_2 oxidation in Run AA-028, whether based on SO_2 decay or aerosol production, was about 7 percent/hr, or *less* than that observed in the absence of the olefin and NO_x pollutants. It appears then that there is no evidence (here) to support or deny the zwitterion theory for SO_2 oxidation in irradiated atmospheres. In the zwitterion theory, there is nothing to explain the SO_2 oxidation rate where very little olefins and O_3 could be detected, or the abrupt decline in SO_2 oxidation where substantial amounts of olefin, SO_2, and O_3 were still present. In authentic smog atmospheres, homogeneous SO_2 oxidation may be very complicated. Energy transfer from important intermediates might play a significant inhibitory role. Zwitterions may well be important intermediates for SO_2 oxidation, but it is also likely that other constituents of smog are competitive with SO_2 for reactions with the diradical.

Influence of Primary Auto-Exhaust Aerosols on Development of Secondary Aerosols

To facilitate experimental control, most smog-chamber studies have been conducted with particle-free air – a condition which is obviously unrealistic compared with urban atmospheres. Results from API project EF-2 at Battelle[11] indicated that primary automobile particulate had a positive effect on the amount of light scattering that developed during irradiation of automobile-exhaust vapors. The changes in light scattering could not be clearly interpreted, however, because techniques were not available for measuring the concentration of suboptical-size particles. In the present program, the effect of preexisting particles on photochemical-aerosol development was reinvestigated, using the MASS in conjunction with auto-exhaust experiments. The concentration of primary aerosol was controlled by filtering the exhaust while adding it to the smog chamber. In some experiments, exhaust was added without filtering. Two series of experiments were conducted in this manner – one at higher primary aerosol concentrations than the other. The different sources of auto exhausts, automobile operations, and methods of transferring exhaust to the smog chamber are described in Appendix A.

Moderate Versus Zero Primary-Aerosol Levels. In the first set of experiments, conducted with an API project EF-8 automobile, carburetor enrichment was used to provide a suitable exhaust HC/NO_x ratio for smog-chamber experiments. This enrichment also provided larger than normal amounts of primary aerosol, such that the total-surface-area concentration of primary aerosol present in the chamber at the outset of irradiation (~1300 $\mu m^2 cm^{-3}$) approached that existing in ambient air in the mornings as photochemical reactions begin.

Results of irradiating auto exhaust in the presence (unfiltered) and absence (filtered) of primary aerosol are shown in Figure 10.* With the exception of the differences in primary aerosol concentration, the experiments were essentially identical, and the ensuing gas-phase reactions which were monitored were also very similar.

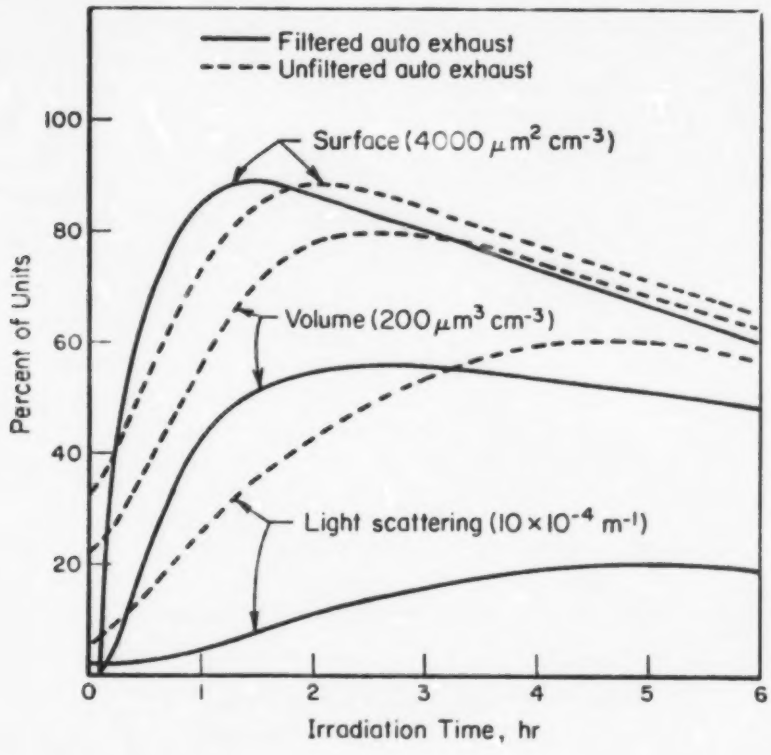

FIGURE 10. EFFECT OF PRIMARY AUTO-EXHAUST PARTICLES ON SECONDARY AEROSOL GROWTH AND LIGHT SCATTERING (16 PPM C HYDROCARBONS)

The two aerosol-volume-concentration curves in Figure 10 indicate that initially the volumetric conversion rates are nearly the same and that, at the end of the irradiation, the difference in total volume is nearly equal to the initial difference, i.e., the volume of primary exhaust aerosol. Therefore, the volume of aerosol formed photochemically is not substantially influenced by the presence of primary aerosol and the large difference occurring in integrated light scattering must be associated with other properties of the aerosols. As indicated in Figure 10, the

*These data and discussion are included in the *Proceedings of the Third International Clean Air Congress* (Reference 1) and in Battelle-Columbus' Interim Report on "Motor Fuel Composition and Photochemical Smog" to the American Petroleum Institute (Reference 10).

initial formation rate of aerosol surface was significantly greater for the filtered exhaust. This observation is consistent with the difference in nucleation rates (not shown in Figure 10); more nuclei were formed and therefore more surface was initially formed in the case of filtered exhaust. As the irradiations progressed, the total surface area concentrations became similar after nucleation subsided.

Light scattering, however, does not depend on the total amount of surface area associated with particles, but rather on the amount of surface area associated with particles >0.2 μm in diameter (not a strict cutoff at 0.2 μm) and increases as the diameter of the particles approach 0.5 μm. Thus the differences observed in light scattering can be explained best by examining the distribution of surface over the aerosol size range.

The distributions at irradiation periods of 0.5 and 4 hours are indicated in Figure 11 for the two auto-exhaust experiments discussed above. (The surface distributions in Figure 11 are dimensioned such that the area under a curve in a given size range is directly proportional to the surface area in that size range.) Upon comparing the surface distribution of the aerosol in the filtered- and unfiltered-exhaust experiments at 0.5 hour, one notes that the total area under the curve in the filtered case is greater than that in the case where particles were present initially. However, the area under the surface curve in the important light-scattering range (>0.2 μm) is much greater for the unfiltered exhaust. Comparison of the results at 4 hours reveals that the amount of surface associated with aerosols in the light-scattering range is again greater for the unfiltered exhaust and that the distribution approaches the size range of optimum scattering efficiency.

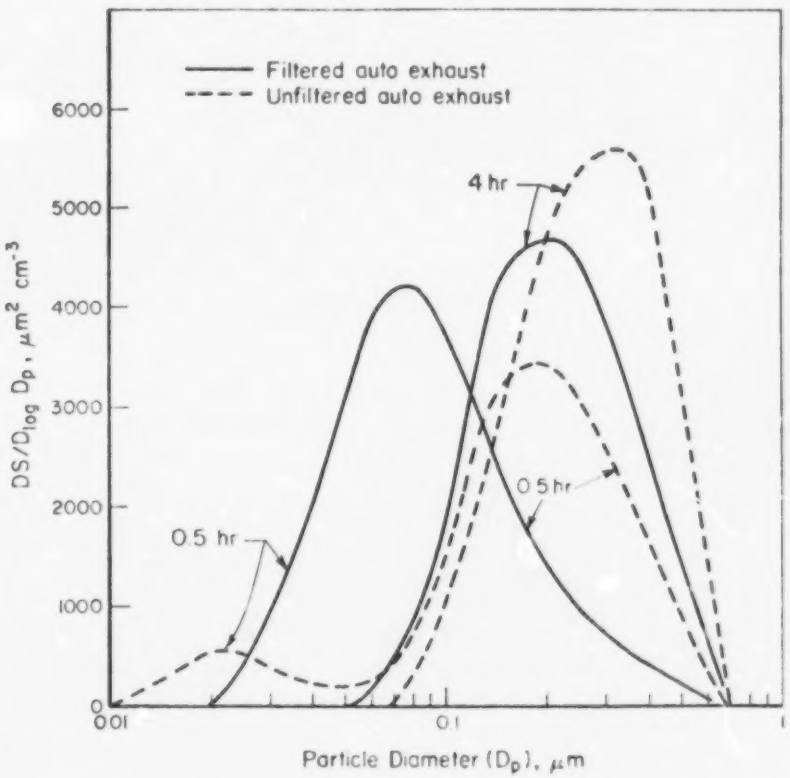

FIGURE 11. EFFECT OF PRIMARY AUTO-EXHAUST PARTICLES ON THE SURFACE DISTRIBUTION OF SECONDARY AEROSOLS (IRRADIATED AUTO EXHAUST, 16 PPM C HYDROCARBONS)

Thus the differences in light scattering observed upon irradiation of filtered and unfiltered auto exhaust can be explained primarily by differences in the resulting aerosol surface distributions rather than by differences in total volume of photochemical aerosols generated.

Low Versus Zero Primary Aerosol Levels. Another series of exhaust experiments was conducted using two similar automobiles, one operating on leaded fuel and the other on nonleaded fuel. The history of these two automobiles, provided by the EPA/CRC Project CAPE-19 committee, is well documented.[18] For these experiments, suitably high HC/NO_x ratios were obtained by adding a synthetic mixture of auto-exhaust hydrocarbons to actual exhausts emitting from the cars operating in their normal configuration. The ratio of synthetic/actual exhaust was 5/3. Because the cars were operated normally and the actual exhaust was diluted with synthetic exhaust, the amounts of primary aerosol present before irradiation were much less than in the preceding experiments using the API automobile. With unleaded fuel, the initial aerosol surface-area concentration was only $\sim 50\ \mu m^2 cm^{-3}$; with leaded fuel, it was $\sim 500\ \mu m^2 cm^{-3}$. Because of the small concentration of primary aerosol, no substantial differences in the size distributions and volume concentrations were observed in comparing the filtered- and unfiltered-exhaust experiments.

As indicated in Table 1, there was no apparent difference in the photochemical reactivity of exhausts derived from leaded or nonleaded fuel. Respective rates of NO oxidation, maximum O_3 and aldehyde concentrations, and the degree of eye irritation were also similar for both types of exhaust.

In conclusion it appears that preexisting (primary) aerosols have little effect on the volume of aerosol material produced by photochemical processes. However, at aerosol surface concentrations similar to those in the atmosphere, suboptical-size aerosols effectively increase the size of the aerosols formed secondarily, which is likely to increase the total amount of light scattering and thus account for observations reported in the EF-2 program.[11]

REFERENCES

(1) Miller, D. F., and Levy, A., "Aerosol Formation in Photochemical Smog: The Effect of Humidity and Small Particles", presented at the Third International Clean Air Congress, Düsseldorf, Germany (October, 1973).

(2) Whitby, K. T., Clark, W. E., Marple, V. A., Sverdrup, G. M., Willeke, K., Liu, B.Y.H., and Pui, D.Y.H., "Evolution of the Freeway Aerosol", presented at the ACS Annual Meeting, Chicago, Illinois (August, 1973).

(3) Whitby, K. T., Wilson, W. E., Pui, D.Y.H., Miller, D. F., Levy, A., Kittelson, D. B., and Cantrell, B. K., "Effect of Stirring on Aerosol Production in a Smog Chamber", presented at the ACS Annual Meeting, Chicago, Illinois (August, 1973).

(4) Miller, D. F, Wilson, W. E., Pui, D.Y.H., Whitby, K. T., and Levy, A., "The Size Distribution and Concentration of Combustion and Photochemical Aerosols Attributable to Automobiles", paper No. 74-151, presented at the 67th Annual Meeting of the Air Pollution Control Association, Denver, Colorado (June, 1974).

(5) Scofield, F., Levy, A., and Miller, S. E., National Paint, Varnish and Lacquer Association, Inc., Circular No. 797 (January, 1969).

(6) Tuesday, C. S., "Chemical Reactions in the Upper and Lower Atmosphere", Interscience, New York, New York (1961).

(7) Pitts, J. N., Jr., Vernon J. M., and Wan, J.K.S., *Intern. J. Air and Water Poll.*, 9, 595-600 (1965).

(8) Gordon, R. J., "Pilot Study of Ultraviolet Radiation in Los Angeles", J. S. Nader (Ed.), National Air Pollution Control Administration, Durham, North Carolina (1967).

(9) Whitby, K. T., Liu, B.Y.H., Husar, R. B., and Barsic, N., Jr., "The Minnesota Aerosol-Analyzing System Used in the Los Angeles Smog Project", J. Colloid Interface Sci., 39, 136 (April, 1972).

(10) Levy, A., Miller, D. F., Hopper, D. R., Spicer, C. W., and Trayser, D. A., "Motor Fuel Composition and Photochemical Smog", Battelle-Columbus Interim Report to the American Petroleum Institute on Project EF-8 Report No. CEA-4 (December, 1973).

(11) Wilson, W. E., Jr., Miller, D. F., Levy, A., and Stone, R. K., *J. Air Poll. Control Assoc.*, 23(11), 949-56 (1973).

(12) Morris, E., and Niki, H., *J. Phys. Chem.*, 75, 3640 (1971).

(13) Demerjian, K. L., Kerr, J. A., and Calvert, J. G., *Adv. in Environ. Sci. and Tech.*, 4 (1973).

(14) Cox, R. A., and Penkett, S. A., Trans. Faraday Soc., I, 68, 1735 (1972).

(15) Clark, W. E., and Whitby, K. T., "Measurement of Aerosols Produced by the Photochemical Oxidation of SO_2 in Air", Particle Laboratory Publication No. 181, University of Minnesota (July, 1972).

(16) Perry, J. H., *Chemical Engineer's Handbook*, 4th Edition, McGraw-Hill, New York (1963), pp 3-79.

(17) Sidebottom, H. W., Badcock, C. C., Jackson, G. E., Calvert, J. G., Reinhardt, G. W., and Damon, E. K., Envi. Sci. & Tech., 6 (1), 72 (January, 1972).

(18) Melton, C. W., Mitchell, R. I., Trayser, D. A., and Foster, J. F., "Chemical and Physical Characterization of Automobile Exhaust Particulate Matter in the Atmosphere", Battelle-Columbus Final Summary Report to the Coordinating Research Council (CAPE 19-70) and the Environmental Protection Agency (Contract No. 68-02-0205) (June, 1973).

APPENDIX A

EXPERIMENTAL METHODS

Automobile Exhaust Generation and Sampling

Chassis Dynamometer Operations

The chassis dynamometer used in this program is a Clayton Model CT-200 with a variable-inertia flywheel assembly capable of simulating vehicle weights from 1500 to 5500 pounds. Automobiles were operated by an automated speed controller actuating servomotors to the brake and accelerator. The speed controller functions as a closed-loop system that varies vehicle speed to match a speed-versus-time program prerecorded on magnetic tape.

A slightly modified version of the 1972 Federal driving schedule was used for the experiments. This driving cycle, often referred to as the LA-4 cycle, consists of 22.8 minutes of acceleration, cruising, deceleration, and idle modes covering 7.5 miles. The Federal Test Procedure requires the test car to be started cold from an overnight soak (at laboratory temperature) and almost immediately started into the cycle. To minimize the danger of engine stall during a run, this procedure was modified by including a preliminary "prep" cycle before the actual exhaust-sampling cycle, and to cool the engine and exhaust system for 45 minutes using an external coolant heat exchanger, an exhaust-system cooling blower, the radiator fan, and a cooling air stream on the choke box, carburetor, and intake manifold. During this 45-minute rapid cooldown, all measured temperatures, with the exception of the oil-sump temperature, were decreased to 80 F or below.

Vehicles and Fuels

Exhausts irradiated in Experiments AA-024 and AA-025 were generated from a 1971 Chevrolet used concurrently on an API program (Project EF-8) at Battelle-Columbus. The API agreed to supply the automobile and fuel for these experiments in exchange for a report on the results. The Chevrolet, a BelAir 4-door sedan equipped with a 350-CID V-8 engine and two-barrel carburetor, had been operated only on unleaded fuel. The original HC/NO ratio of the car's exhaust was too low for practical smog-chamber experimentation. Therefore, a "California camshaft" was installed and the main carburetor jets (0.058-inch bore) were replaced with jets of larger bore (0.067 inch). As documented in the EF-8 program[10], these modifications had little or no effect on the hydrocarbon composition of the exhaust, but increased the total hydrocarbon, CO, and aerosol emissions. Fuel used in both experiments was API No. 13A (nonleaded) consisting of 51 percent paraffins, 13 percent olefins, and 32 percent aromatics by weight.

For experiments AA-032 through AA-038, two similar 1970 Fords were used for generating exhaust from leaded and nonleaded fuel. The history of these cars has been carefully monitored for comparing leaded- versus nonleaded-fuel effects on primary particulate emissions.[18] Both cars are Fairlane two-door hardtops equipped with 351 CID V-8 engines, and two-barrel carburetors. Operation of these cars on the chassis dynamometer was the same as that described

above for the API vehicle. The CRC-CAPE-19 fuels, with and without TEL additive (2.45 g Pb/gal), consisted of 63 percent paraffins, 6 percent olefins, and 29 percent aromatics by weight. No modifications were made to these cars to increase the HC/NO ratio. Instead, synthetic-exhaust hydrocarbons were added to the actual exhaust to increase the ratio for the smog-chamber experiments.

Sample Transfer

The goal in auto-exhaust sampling is to produce and transport to the smog chamber an emission sample reasonably representative of vehicle emissions on roadways. The exhaust-sampling facility used on this program is shown schematically in Figure A-1. An exhaust-diverter valve (between the tailpipe of the car and the dilution tunnel) controls the period when the exhaust gases are passed through the tunnel. The dilution tunnel was designed to rapidly quench and thoroughly mix the exhaust gases with clean filtered air, and to establish a flat and reproducible velocity profile at the sampling position. The tunnel is constructed of stainless steel (11-1/2 inches in diameter and 20 feet long), and includes a charcoal filter, an absolute filter, and a mixing orifice at one end and a sampling tube and CVS (constant-volume-sampling) system at the other end. The CVS system induces the dilution-air and exhaust-gas flow through the tunnel. The unit is an Olson Laboratories Model No. 45A-R3 with a four-speed pump motor. During all exhaust-sampling runs the total flow rate was 340 scfm. The volume flow rate of exhaust into the tunnel varied from 15 to 150 cfm. The average dilution-air/exhaust-gas ratio over the entire driving cycle is about 10/1. In an effort to increase this ratio, thereby minimizing the coagulation rate of primary aerosols, an exhaust splitter was installed which diverted only one-fourth the exhaust into the tunnel. This dilution procedure (yielding an average ratio of 40/1) was used on Runs AA-033, AA-035, and AA-036.

As illustrated in Figure A-1, a portion of the diluted exhaust is delivered from the near end of the tunnel to a Teflon holding bag (550-cu ft capacity) contained in a rigid box. During collection, near-isokinetic flow from the tunnel to the bag is achieved by maintaining a constant subatmospheric pressure on the bag. At the conclusion of the driving cycle, the contents of the bag are passed to the smog chamber by applying super-atmospheric pressure on the bag.

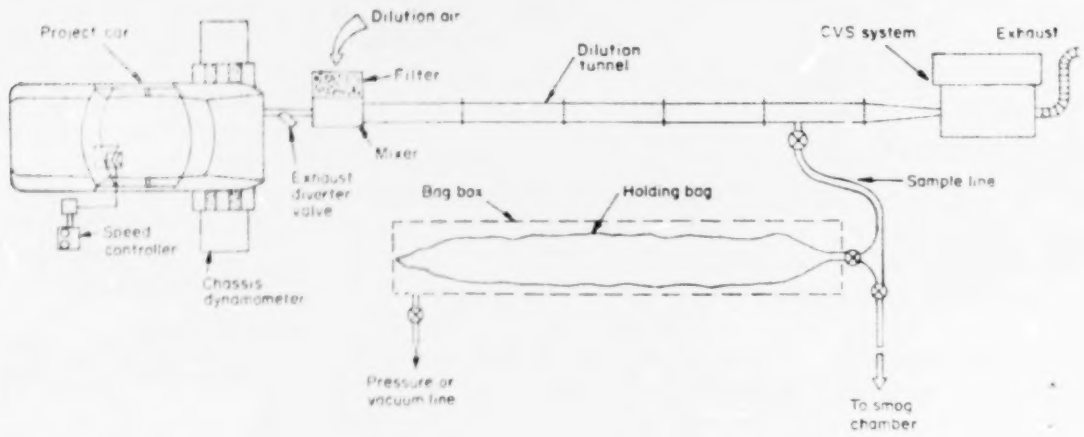

FIGURE A-1. SCHEMATIC OF LABORATORY FACILITY FOR GENERATING AND SAMPLING AUTO EXHAUST

For experiments where the total exhaust flowed into the dilution tunnel (Runs AA-024, AA-025, AA-032, AA-034, AA-037, and AA-038), rapid coagulation of primary aerosol was forestalled by filling the bag half full of filtered air before introducing the exhaust emission. Despite only moderate increase in overall dilution (20/1 rather than 10/1), this technique is fairly successful because the emission associated with the first few minutes of the driving cycle and containing the greatest amount of aerosol is initially diluted manyfold.

Obviously, actual roadway operation of an automobile provides dilution of exhaust more rapidly than can be provided practically in the laboratory, where constant volume sampling and other experimental constraints are imposed. At the overall dilution ratio of 20/1, the cumulative coagulation of primary aerosols (nonleaded fuel combustion) occurring during the 23-minute driving cycle resulted in a unimodal distribution of aerosol surface, with the mode occurring at a particle diameter of 0.1 μm.

Diluting 40/1 in the dilution tunnel resulted in a bimodal distribution of aerosol surface, the major mode occurring at a particle diameter of 0.03 μm and a minor mode at about 0.3-μm diameter.

Dr. Whitby and his colleagues have recently demonstrated that the major mode in the surface distribution of primary auto-exhaust aerosols having undergone dilution along otherwise unpolluted highways is near 0.02 μm.[2] Size-distribution measurements (MAAS) taken directly in Battelle's dilution tunnel confirm that the initial mode in the size distribution is near 0.02 μm, and that the growth in particle size upwards from 0.02 μm is due to the coagulation of aerosols during the collection period. The lifetime of these very small aerosols in urban atmospheres and in heavily trafficked areas is uncertain and will depend on many factors, including particle concentration, turbulence, and the rate of photochemical activity.

Eye-Irritation Measurements

Measures of eye irritation were made by a 24-member eye-panel team chosen from Battelle-Columbus staff. Panelists selected were distributed among three 7-member teams (plus an alternate) according to their responses to three chemical systems:

(1) Clean air (with lights on during eye test)

(2) 2-butene (4 ppm), NO (1.1 ppm), NO_2 (0.9 ppm) - irradiated

(3) Toluene (4 ppm), NO (1 ppm), NO_2 (1 ppm) – irradiated.

The last two systems were selected to expose the panelists to PAN and presumable PbzN, respectively, as well as to significant levels of formaldehyde. The formaldehyde levels in these two reactions were 0.7 ppm in the trans-2-butene system and 0.1 ppm in the toluene system. Response times of the panelists were as follows:

	Clean Air	Trans-2-Butene	Toluene
Mean Time, equivalent sec	342	66	82
Index	0.28	7.8	7.5

The mean time in equivalent seconds is defined as the antilog of the geometric-mean response time. The index is defined as 10[(360-t)], where t is the response time. Maximum exposure time was 360 seconds.

For all experiments with auto exhaust, two teams (14 panelists) were exposed during the fifth hour of irradiation. For most experiments with specific hydrocarbons and synthetic exhaust, panelists were exposed about 2 hours after the time of maximum NO_2 concentration. One team of panelists was seated for all experiments. The other two teams alternated from experiment to experiment.

Detailed data of all eye-panel measurements made in this program are presented in the supplementary Data Report. An example of the eye-data tabulation for one experiment (AA-032) is shown below.

RUN AA-032 5/9/73 (3:15) FUEL RE-141B

EYE IRRITATION RESPONSES AND INDICES

NAME	N	P	T	LOG(T)	INDEX A	SEVERITY INDEX
DICK CLARK	10	4	52.	1.716	8.56	2
WALT CHAPIN	15	1	143.	2.155	6.03	1
JOE FOTI	13	2	207.	2.316	4.25	2
BOB CONLON	16	5	190.	2.279	4.72	1
RAY DODDS	2	6	360.	2.556	0.00	0
CHARLES BURLEY	4	3	35.	1.544	9.03	3
WERNER MARGARD	21	7	205.	2.312	4.31	1
BOB LITTLE	6	6	105.	2.021	7.03	1
MARGARET BELL	23	7	124.	2.093	6.56	1
KAY FAMCETT	25	4	236.	2.373	3.44	1
HERB RICKMAN	27	2	157.	2.196	5.64	1
BILL KEELEY	11	5	141.	2.149	6.08	2
PAULINE FAUTH	3	3	42.	1.623	8.33	0
URSEL MCKITRICK	12	1	124.	2.093	6.56	1

COMPUTATIONS

MEAN	151.	2.10	5.79	1.4
ST.DEV.(PANELIST),S	97.	0.29	2.40	
ST.ERROR(PANEL),S/SQ.RT.(14)	23.	0.03	0.64	

EQUIVALENT SECONDS
MEAN 126.

N DENOTES PANELIST NUMBER
P DENOTES PANELIST POSITION AT THE CHAMBER
T DENOTES RESPONSE TIME IN SECONDS
LOG(T) DENOTES BASE 10 LOG OF RESPONSE TIME
INDEX A = 10 * (360 - T)/ 360
SEVERITY INDEX IS A 0-3 RATING OF THE IRRITATION BY THE PANELIST

Reproduced from best available copy.

APPENDIX B

SUMMARY OF AEROSOL COLLECTIONS

TABLE B-1. SUMMARY OF AEROSOL COLLECTIONS BY FILTRATION

Run	Sample Description[a]	Type of Filter	Sampling Time, min	Sample Volume, ft^3	Weight Gain, mg	Disposition[b]
AA-005	Toluene-NO_x	4-in. glass	–	388	10.1	BCL
AA-006	Toluene-NO_x	4-in. glass	–	353	11.1	BCL
AA-007	Toluene-NO_x	4-in. glass	–	392	3.1	BCL
		Gold disk	25	8.8	–	Ditto
		1-in. glass	25	8.8	–	"
AA-008	1-heptene-NO_x	4-in. glass	–	370	1.9	BCL
AA-009	1-heptene-NO_x	4-in. glass	–	382	0.7	BCL
AA-010	1-heptene-NO_x	4-in. glass	–	315	0.7	BCL
AA-011	Benzene-NO_x	4-in. glass	–	338	1.1	BCL
AA-012	Toluene-mesitylene-NO_x	4-in. glass	–	360	3.4	BCL
		Gold disk	30	10.5	–	Ditto
		1-in. glass	30	10.5	–	"
AA-015	Benzene-NO_x-SO_2	4-in. glass	–	374	1.5	BCL
AA-016	SO_2	4-in. glass	–	374	1.8	BCL
AA-019	Propylene-O_3-SO_2-dark	4-in. glass	–	435	3.2	BCL
		Nuclepore	42	6	–	Ditto
AA-020	α-Pinene-NO_x	Nuclepore	42	6	–	BCL
		Gold disk	30	7.1	–	Ditto
		1-in. glass	30	7.1	–	"
AA-021	1-heptene-O_3-dark	4-in. glass	–	430	0.8	BCL
		Nuclepore	27	10	–	Ditto
		Gold disk	30	10.5	–	"
		1-in. glass	30	10.5	–	"
AA-022	1-heptene-O_3-SO_2-dark	4-in. glass	–	500	4.0	BCL
		Nuclepore	28	10	–	Ditto
		Gold disk	30	10.5	–	"
		1-in. glass	30	10.5	–	"
AA-023	Toluene-NO_x-CN	4-in. glass	–	346	–	BCL
		Nuclepore	30	10	–	Ditto
AA-024	Auto exhaust – smog	4-in. glass	–	374	1.7	BCL
		Nuclepore	30	10	–	Ditto
		Silver	26	10	–	"
	Auto exhaust – primary	Nuclepore	22	22	–	"
		Silver	22	22	–	"
AA-025	Auto exhaust – smog	4-in. glass	–	385	1.4	BCL
		Nuclepore	7	7	–	Ditto
		Silver	7	7	–	"
	Auto exhaust – primary	Nuclepore	30	10	–	"
		Silver	22	11	–	"

TABLE B-1. (Continued

Run	Sample Description[a]	Type of Filter	Sampling Time, min	Sample Volume, ft^3	Weight Gain, mg	Disposition[b]
AA-028	1-heptene-NO_x-SO_2	4-in. glass	46	313	0.9	BCL
		Nuclepore	30	10	–	EPA
		1-in. glass	25	9	–	BCL
		Millipore	53	–	0.004	EPA
		Silver	16	10	–	EPA
AA-029	1-heptene-NO_x-SO_2	4-in. glass	47	317	0.75	BCL
		Nuclepore	66	21	–	EPA
		1-in. glass	46	16.5	–	BCL
		Millipore	55	–	–0.002	EPA
		Silver	17	10	–	EPA
AA-030	1-heptene-NO_x	4-in. glass	53	342	0.5	BCL
		Nuclepore	63	21	–	EPA
		1-in. glass	30	10.8	–	BCL
		Millipore	61	–	0.007	EPA
		Silver	17	10	–	EPA
AA-031	1-heptene-NO_x-CN	4-in. glass	51	334	0.59	BCL
		Nuclepore	56	20	–	EPA
		1-in. glass	28	10	–	BCL
		Millipore	60	–	0.004	EPA
		Silver	20	11	–	EPA
AA-032	Auto exhaust-CN	4-in. glass	52	338	0.56	BCL
		Nuclepore	56	20	–	EPA
		1-in. glass	31	10	–	BCL
		Millipore	62	–	0.022	EPA
		Silver	17	10	–	EPA
AA-033	Auto exhaust	4-in. glass	51	327	0.54	BCL
		Nuclepore	56	20	–	EPA
		1-in. glass	31	11	–	BCL
		Millipore	66	–	0.015	EPA
		Silver	16	10	–	EPA
	Before irradiation	Ab-Nuclepore	–	2	–	EPA
	After irradiation	Ab-Nuclepore	–	5	–	EPA
AA-034	Auto exhaust – filtered	4-in. glass	52	355	0.47	BCL
		Nuclepore	55	20	–	EPA
		1-in. glass	26	9	–	BCL
		Millipore	65	–	0.005	EPA
		Silver	16	10	–	EPA
AA-035	Auto exhaust (leaded)	4-in. glass	56	348	0.42	BCL
		Nuclepore	57	25	–	EPA
		1-in. glass	34	12.2	–	BCL
		Millipore	65	–	0.005	EPA
		Silver	16	10	–	EPA

TABLE B-1. (Continued)

Run	Sample Description[a]	Type of Filter	Sampling Time, min	Sample Volume, ft^3	Weight Gain, mg	Disposition[b]
AA-036	Auto exhaust (leaded)	4-in. glass	50	334	0.36	BCL
		Nuclepore	46	20	–	EPA
		1-in. glass	38	13.6	–	BCL
		Millipore	66	–	0.017	EPA
		Silver	26	12	–	EPA
	Before irradiation	Ab-Nuclepore	–	2	–	EPA
	After irradiation	Ab-Nuclepore	–	5.5	–	EPA
AA-037	Auto exhaust (leaded) – filtered	4-in. glass	61	369	0.43	BCL
		Nuclepore	74	25	–	EPA
		1-in. glass	32	11.5	–	BCL
		Millipore	62	–	0.022	EPA
		Silver	20	10	–	EPA
AA-038	Auto exhaust (leaded) – filtered	4-in. glass	49	349	0.45	BCL
		Nuclepore	71	24	–	EPA
		1-in. glass	32	11.5	–	BCL
		Millipore	64	–	0.008	EPA
		Silver	18	10	–	EPA

(a) Experimental conditions. Unless otherwise indicated, all aerosol samples were withdrawn from the smog chamber after irradiation.

(b) EPA; filters mailed to Project Officer at EPA. BCL; filters retained at Battelle's Columbus Laboratories.